SANDIA REPORT

SAND97–2786 • UC–704
Unlimited Release
Printed November 1997

High Power Ion Beam (HPIB) Modification of One- and Two-Layer Metal Surfaces

T. J. Renk, N. R. Sorensen, D. Cowell Senft, R. G. Buchheit,
M. O. Thompson, K. S. Grabowski

Prepared by
Sandia National Laboratories
Albuquerque, New Mexico 87185 and Livermore, California 94550

Sandia is a multiprogram laboratory operated by Sandia Corporation, a Lockheed Martin Company, for the United States Department of Energy under Contract DE-AC04-94AL85000.

Approved for public release; further dissemination unlimited.

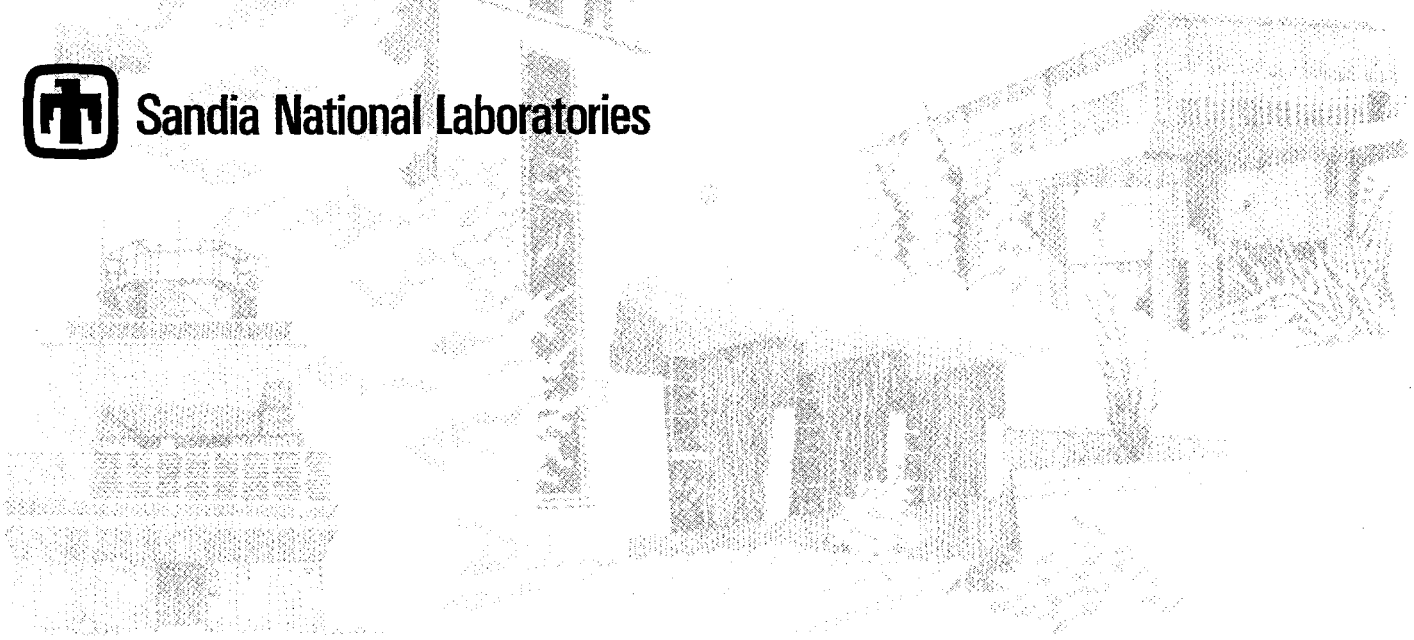

Sandia National Laboratories

Issued by Sandia National Laboratories, operated for the United States Department of Energy by Sandia Corporation.

Available to DOE and DOE contractors from
Office of Scientific and Technical Information
P.O. Box 62
Oak Ridge, TN 37831

Prices available from (615) 576-8401, FTS 626-8401

Available to the public from
National Technical Information Service
U.S. Department of Commerce
5285 Port Royal Rd
Springfield, VA 22161

NTIS price codes
Printed copy: A03
Microfiche copy: A01

SAND97-2786
Unlimited Release
Printed November 1997

Distribution Category
UC-704

High Power Ion Beam (HPIB) Modification of One- and Two-Layer Metal Surfaces

T. J. Renk
Beam Applications and Initiatives Department

N. R. Sorensen, D. Cowell Senft
Materials Aging & Reliability: Interfaces Department

Sandia National Laboratories
P. O. Box 5800
Albuquerque, NM 87185-1182

R. G. Buchheit
The Ohio State University
Department of Materials Science and Engineering
Columbus, OH 43210-1187

M. O. Thompson
Department of Materials Science
Cornell University, Ithaca, NY 14853

K. S. Grabowski
Naval Research Laboratory
Washington, DC 20375

Abstract

Intense pulsed high-power ion beams have been demonstrated to produce enhanced surface properties by changes in microstructure caused by rapid heating and cooling of the surface. Additional improvements can be effected by the mixing of a previously deposited thin-film layer (surface alloying or ion beam mixing) into any number of substrate materials. We have conducted surface treatment and alloying experiments with Al, Fe, and Ti-based metals on the RHEPP-1 accelerator (0.8 MV, 20 W, 80 ns FHWM, up to 1 Hz repetition rate) at Sandia National Laboratories. Ions are generated by the MAP gas-breakdown active anode, which can yield a number of different beam species including H, N, and Xe, depending upon the injected gas. Enhanced hardness and wear resistance have been produced by treatment of 440C stainless steel, and by the mixing of Pt into Ti-6Al-4V alloy. Mixing of a thin-film Hf layer into Al 6061-T6 alloy (Al-1.0Mg-0.6Si) has improved its corrosion resistance by as much as four orders of magnitude in electrochemical testing, compared with untreated and uncoated Al6061. Experiments are ongoing to further understand the microstructural basis for these surface improvements.

Table of Contents

High Power Ion Beam (HPIB) Modification of One- and Two-Layer Metal Surfaces

I. Introduction

Metallic alloys of commercial interest are generally formed to optimize desired bulk properties like strength and ductility. Such bulk optimization can compromise surface properties such as corrosion resistance. As an example, second-phase particles in the bulk act to pin dislocations and hence increase hardness, but these particles on the surface can act as initiation sites for corrosion. A desirable post-treatment of alloys would preserve bulk properties, but modify the surface to optimize surface properties.

Pulsed irradiation of surfaces by high power ion beams can provide such a treatment. Fig. 1 schematically illustrates the process. A beam of ions impinges on a metal surface from the left. The ions penetrate in depth, and beam energy is converted to thermal energy, producing a rapid melt zone. The pulse length is long enough for thermal diffusion to increase the melt depth beyond the ion range. Heat conduction into the substrate leads to resolidification at quench rates that can exceed 10^9 K/s. This rapid cooling can lead to the formation of non-equilibrium surface microstructures and metastable alloys not accessible by conventional alloying methods. Because the voltage typically falls through the power pulse, energy deposition is almost uniform with depth down to the ion range, which can be as high as 10 μm for 750 kV protons impinging on Al. The ion range can be adjusted by selecting different ions for acceleration, as will be detailed below.

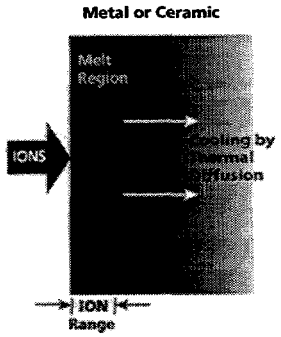

Figure I. Schematic View of IBEST process.

The types of surface improvement produced by this process include increased surface hardness and resistance to corrosion. Additional alloying elements can be added to the surface by the application of a separate thin-film layer to the substrate prior to beam treatment. During the power pulse, this film diffuses or convects into the substrate. The coating can be chosen to produce substantial improvements in surface properties beyond that possible by either conventional alloying or by intense beam treatment without the coating layer. This process can be referred to as surface alloying or ion beam mixing.

Both surface modification and alloying with intense ion beams were originally demonstrated in the former Soviet Union[1] and at Cornell University.[2] The process discussed here is known as Ion Beam Surface Treatment (IBEST), and further details are given elsewhere.[3] The treatment experiments discussed here were undertaken on the RHEPP 1 facility at Sandia National Laboratories (0.8 MV, 20 W, 80 ns FWHM, up to 1 Hz repetition rate).

The ions are generated by the MAP (Magnetically confined Anode Plasma) gas-breakdown ion source operated in a magnetically insulated ion diode.[4] In such a diode, ions are accelerated across an applied voltage, while electron generation is inhibited by a transverse magnetic field. The ion source is an injected gas puff which is then ionized. The accelerated ions for any given treatment are selected both on the basis of model-derived parameters such as ion stopping range, and on empirically-derived effects such as processed surface smoothness. We have produced beams using H, He, CH_4, N, O, Ar, Kr, and Xe gas injection. Typical beam parameters used in the work reported here are a maximum voltage of 750 kV, current densities ≤ 250 A/cm^2, pulse durations on target < 1 μs, and beam fluences ≤ 10 J/cm^2.

The experiments discussed here demonstrate a proof-of-principle. Repetitively pulsed ion beams are a scalable technology that operate at a high net electrical efficiency, with the potential for yielding industrially viable processing. Compared with ion implantation, costs can be significantly less expensive. In addition, the process here is fundamentally pulsed and thermal in nature, compared to the typically room-temperature implantation process. Each pulse delivers ~ 10^{13} ions/cm^2, so unless many pulses are used, implantation effects are negligible. Compared to electron beam processing, while the energy deposition profile and electrical efficiency can be similar, to produce a comparable melt range the electron voltage must be held below 50 kV. The dynamics of electron beam diodes makes it difficult to produce and transport 100 A/cm^2 at 50 kV.

Experiments with high-power ion beams have previously demonstrated improvements in corrosion resistance of both Al- and Fe-based alloys,[3] mainly by the reduction of second-phase particles in the rapidly melted layer. But it is also known[5] that, for example, in the case of aluminum, addition of small amounts of transition metals such as Zr and Nb can lead to improvements in corrosion resistance. These metals are almost insoluble in aluminum under equilibrium conditions. However, we discuss below the result of applying thin-film coatings of these metals and mixing them into the substrate. For these experiments, the coatings have been sputter-deposited either in pure form or as a "co-sputtered" alloy. In the latter case, two sputter guns are operated simultaneously, one emitting the candidate coating, the other the elemental substrate metal in a predetermined ratio. We are also investigating other less costly methods of applying the thin-film coating. The advantage of ion beam mixing over standard thin-film deposition alone is that the beam processing grades the coating into the substrate, effectively eliminating the interface between coating and substrate. Thus IBEST processing can be superior to sputter-deposited films alone, because of the adhesion problem associated with the high stresses inherent in such films, which limit their thickness to ~ 0.5 μm. Successful mixing should result in an inherently stronger bond with the underlying substrate.

For this report, we discuss surface treatment of 440C stainless steel (no mixing) resulting in improved hardness and wear durability. We also detail mixing experiments where binary alloys were formed by sputter deposition of 0.06 to 4 μm layers on both Al and Ti. For Al, the overcoat layers were of Cr and Hf. Nb and Pt were the overcoat layers tested on Ti. Typical sample size was either a 2 cm disk, or a 1 x 5.5cm strip. After RHEPP-1 treatment, the Al samples were subjected to electrochemical impedance corrosion tests. Hardness was measured by nanoindentation, and tribological testing was by a linear recip-

rocating tribometer using a ball-on-flat geometry. Samples exhibiting performance gain were studied by scanning electron microscopy (SEM), x-ray diffraction (XRD), and Rutherford Backscattering Spectrometry (RBS) to gain further microstructural understanding, and for comparison of inferred treatment effects with modelling code predictions. The experimental setup, description of the beam, and diagnostic studies of the samples produced are discussed below.

II. Experimental Setup

Figure 2 shows the treatment geometry. An annular beam of average radius 10 cm is generated from a magnetically insulated ion diode, and propagates to a target table located between 25 and 65 cm away. Insulation coils located on the cathode side suppress electron leakage current. The MAP ion source consists of an axially located plenum valve and inner and outer flux excluders. Prior to the power pulse, the valve is energized, and gas expands radially towards the annular space between the flux excluders. A fast coil is pulsed which ionizes the gas, and the interaction of the fast coil magnetic field with the slower insulation field pushes the resulting plasma into position for acceleration when the power pulse arrives. A set of magnetically insulated Faraday cups (outfitted with permanent magnets) is mounted on the target table. The cups measure the total beam fluence as a function of position, and in addition are able to resolve different beam constituents through time-of-flight (TOF) analysis. For instance, nitrogen injection produces a three-component beam that is initially protonic (about 10% of total fluence), followed by twice- and singly-ionized nitrogen. Surface processes as well as gas breakdown mechanisms appear to contribute to the beam generation process. As an example, when Xe is injected, part of the beam is composed of several charge states of C. The injected gas species is chosen by observed effects on treated samples. Nitrogen beams produce a smoother surface topology compared to proton beams, for instance.

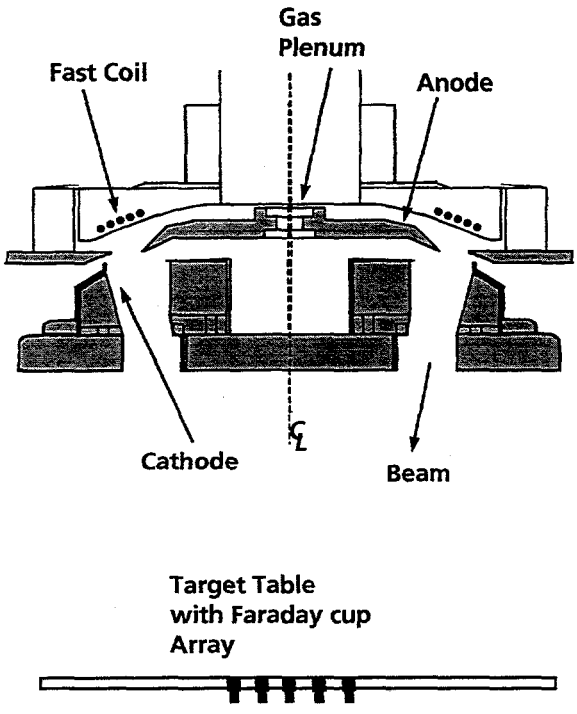

Figure 2 Diode Geometry including MAP ion source and treatment area.

An alternative source used on some experiments is the more familiar epoxy-filled groove or "flashover" anode. The grooves are located in place of the annulus defined by the inner and outer flux excluders. When the power pulse arrives, the triple-point stress at the corners of the grooves breaks down, leading to the formation of a dense plasma from which the beam is extracted. The beam is initially composed of protons (about 30% of the total), then carbon for the remainder of the pulse. Samples for treatment were located near the Faraday cup locations so that depositional fluences could be determined.

Waveforms of the beam voltage and current density incident upon the samples could be input to a Code modeling the temperature response. Other input parameters include the thermal conductivity, heat of fusion, and specific heats for both overcoat and substrate materials. The Code includes the effect of 1-D heat diffusion, but not hydrodynamic or ablation effects. We attempted to operate in a fluence regime lower than that predicted for vaporization of the overcoat material, which should minimize ablation. The Code then yielded the surface temperature and melt depth of the substrate as a function of time (the thin overcoat thickness ensured their complete melting).

III. Treatment of 440C Martensitic Stainless Steel

This type of stainless steel was chosen for study because of its commercial importance as a bearing steel. Unlike the other treatments described below, these samples were not overcoated.

Samples were treated by the mixed species beam from the flashover diode at various fluence levels. They were then subjected to nanoindentation hardness testing, as well as reciprocating tribometer cycles to measure the evolution of surface friction coefficient with time. Figs. 3a and 3b show 2000X SEM views of the surface before and after treatment. The round-shaped gray areas in Fig. 3a are second-phase particles, predominantly of chromium carbide. These are largely missing in the IBEST-treated surface. Fig. 3b shows a lath martensitic microstructure. (The small dark spots in the treated image are actually depressions of approximate depth 1 μm.) A quantitative image analysis of these and other SEM scans yields an average inclusion size of 0.93 μm prior to treatment, with the largest inclusion 7.83 μm in diameter. After treatment at 4

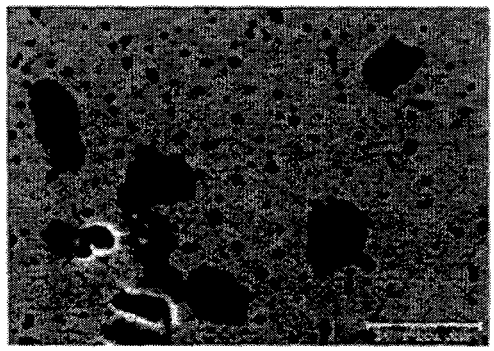

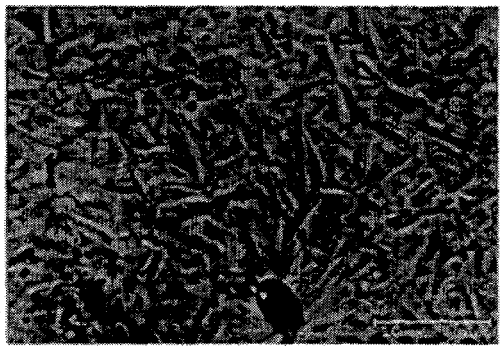

Figures 3a (top) and 3b (bottom) Scanning electron images, magnified 2000 times, showing surface of 440C stainless steel before(top) and after (bottom)beam treatment

J/cm^2 the numbers are 0.51 μm and 1.02 μm, respectively, and these latter measurements are of the depressions mentioned above. The IBEST process has thus led to considerable dispersal of the carbide inclusions. Fig. 4 indicates that surface hardening increases as a function of beam fluence. Examination of wear tracks indicates an increased ability of the treated 440C to resist wear compared to untreated 440C. We believe that this is due to the carbide dispersal produced by IBEST.

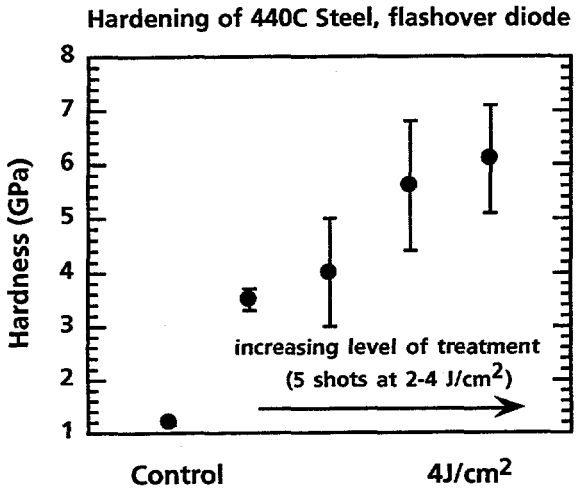

Figure 4 Surface hardening, as measured by nanoindentation, for 440C Stainless Steel as a function of beam fluence. Samples treated by flashover diode.

IV. Mixing of transition metals into Al 6061-T6 to improve corrosion resistance

Pure Al is highly corrosion-resistant, but unusable for most commercial applications because of its poor mechanical properties. Conventional alloying elements such as Cu, Mg, and Si can add strength, but second phase particles formed during slow solidification and subsequent heat treatment can serve as initiation sites for corrosion. We have applied thin-film coatings of a number of transition metals (Zr, Cr, Hf) over Al 6061-T6, a standard commercial Al alloy. The samples were treated by beams from various input gases and fluences. Small areas of treated samples were then immersed in a 0.5 M NaCl solution for varying periods of time up to 24 hours. During exposure, electrochemical impedance spectra were generated and the polarization resistance R_p was determined as a function of time. The higher the value of R_p, the lower the rate of corrosion.

Fig. 5 shows a plot of measured polarization resistance R_p, in units of ohm-cm^2, as a function of time for a thin-film Hf-coated Al 6061 sample which showed particularly good corrosion resistance at the highest treatment fluence tested. The sample was positioned so that a range of fluences was sampled during the same shot sequence. Treatment was with the MAP nitrogen beam. There are five sample areas labeled L0, L1, M, R1, and R0 in increasing fluence, with the peak fluence (R0) approximately 4 J/cm^2. For reference, also shown are the R_p values of 1) base Al 6061 with no coating or treatment, and 2) a Hf-coated but untreated sample. We have previously confirmed that treatment of Al 6061 without added coatings does not lead to any improvement in corrosion resistance. In addition, previous tests of untreated 99.999% Al yield R_p values in the 10^6 range.

Notice that the measured polarization resistance increases with increasing fluence on this sample. In addition, the peak polarization resistance (10^8 ohm-cm^2) seen on the treated Hf-coated sample exceeds that measured for the base Al 6061 by 4 orders of magnitude, and exceeds both the uncoated/untreated Hf and 99.999% Al samples by two orders of magnitude. Thus we have substantially improved the corrosion resistance of Al 6061 alloy by mixing of a thin-film Hf layer into the substrate. Note also that the treatment can *lower* the corrosion resistance of the sample, as seen from the lowest level of fluence shown (L0). This results in a lower R_p value than that measured for the base Al 6061. Further analysis is planned to understand the microstructural basis for these results.

RBS measurements of previous Hf-coated samples are consistent with migration of the Hf to a depth of at least 6.5μm, consistent with both modeling code predictions of

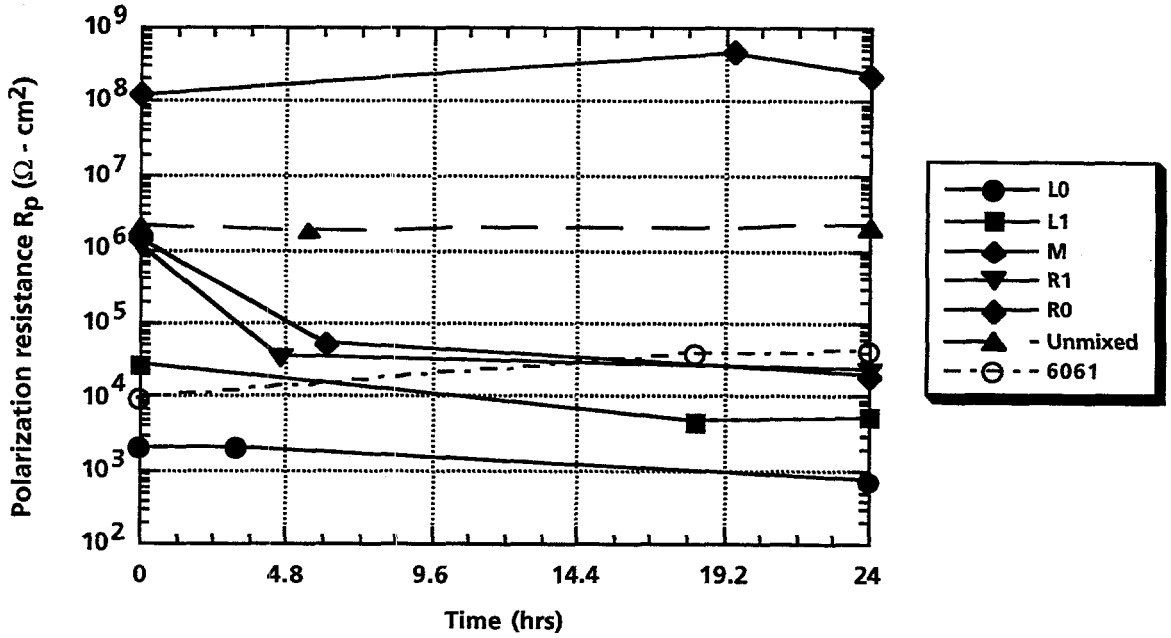

Figure 5. Polarization resistance R_p measured as a function of time for a Hf-coated Al6061 sample for 5 different fluences.

the beam-generated melt depth, and with measured melt depths of cross-sectioned samples. Since this length exceeds that possible by liquid-phase diffusion only, this implies that the Hf migrates into the molten Al by convective processes during the power pulse.

We have measured similar although not as consistently high levels of polarization resistance with mixed thin-film Cr and Zr coatings.

V. Mixing of Pt into Ti alloys to increase corrosion and wear resistance

Titanium is used for industrial applications in a number of alloys, including "commercially pure" (99.2%). Its corrosion resistance is quite good, but wear resistance can be a problem. A thin (~ 200 Å) hard layer of TiO_2 forms on Ti under normal atmospheric conditions, but if this layer is penetrated in a wear application, galling and micro-welding can result, leading to a compromise of surface integrity.

In an attempt to improve the tribological performance of titanium, a co-sputtered layer of 90 at% Ti and 10 at% Pt with a total thickness of 1 μm was coated on Ti-6Al-4V (Ti Grade 5), a common industrial titanium alloy. After treatment with the MAP nitrogen beam, the sample was tested in the tribometer to measure the friction coefficient as a function of the number of wear cycles. The counterface used was a 440C steel ball. The samples were tested at a contact pressure of 0.9 GPa and a velocity of 0.17 cm/s. An untreated sample of Ti-6Al-4V and a sample that was coated with the Ti-Pt layer but untreated were tested under identical conditions for comparison. Figure 6 shows typical friction coefficient traces for all three samples. Note that the friction coefficient rises rapidly for both the untreated Ti sample and the coated but untreated sample after about only 20 cycles, indicating deterioration of the surface integrity and the build-up of wear debris. The dura-

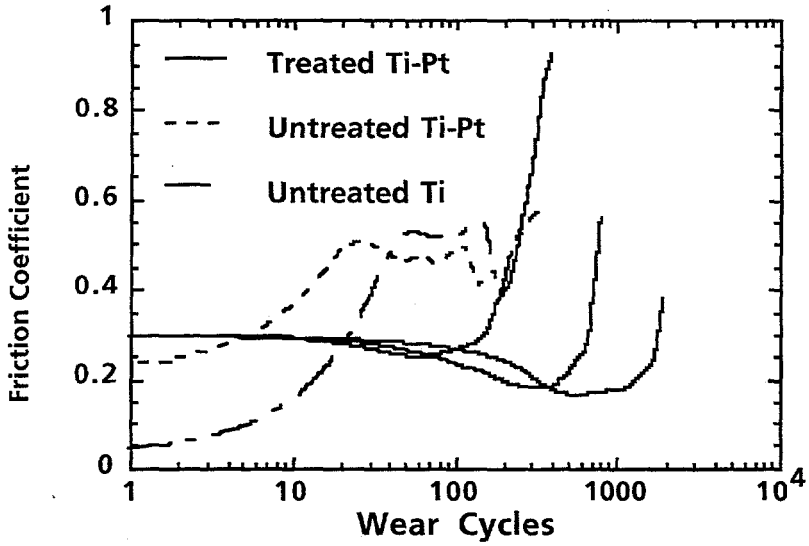

Figure 6. Friction coefficient as a function of wear cycles for untreated Ti-6Al-4V, Pt-coated but untreated Ti, and treated Pt-Ti layer (3 cases)

tion of low friction coefficients for the treated Ti-Pt sample shows a large variation. We think this variation is due to the local nature of the tribometer test. Beam-induced surface roughening and/or topological imperfections such as microcraters may affect individual tests, depending upon where on the sample the tribometer is operating. In one case the friction coefficient is maintained below 0.3 for 1800 cycles which is an improvement over untreated Ti of two orders of magnitude. Figure 7 shows SEM micrographs of the wear tracks for untreated, coated Ti-Pt (Fig. 7a) and treated Ti-Pt (Fig. 7b). Wear scars are much more prominent in the untreated case, indicating that treatment and mixing of the surface produces a reduction in the wear rate. For comparison, treated Ti-5 samples have exhibited low friction coefficients for between 200 and 500 cycles, an improvement upon the untreated case, but not as good as with the Pt mixture.

RBS studies of other Pt-Ti mixing

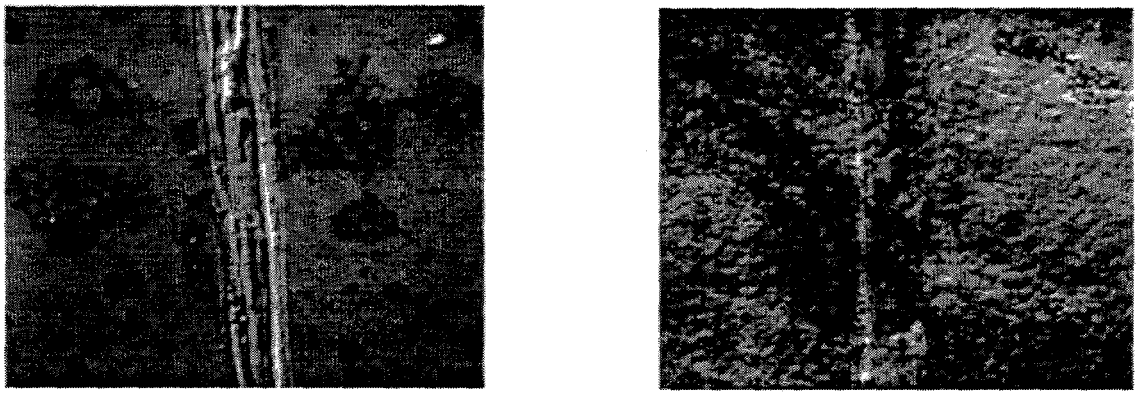

Figures 7a and 7b. Scanning electron images, showing Tribometer-caused wear tracks in Pt-Ti co-sputtered layer without beam treatment (left, magnified 300 times), and a sample are of treated layer that withstood 2000 wear cycles (right, magnified 200 times).

samples indicate migration of the Pt into the substrate by convective processes well beyond the original coating thickness. Measurements of a treated pure Pt layer of initial thickness 0.18μm show surface Pt concentrations in the 25-30 atomic percent range, and declining with depth but still with significant Pt concentrations to beyond 1 μm depth. This illustrates the ability of IBEST-induced surface alloying to grade the coating layer into the substrate substantially beyond the original coating thickness. XRD measurements indicate minimal conversion of the original α-phase Ti to β-phase after treatment, with a number of new lines present that are not consistent with known Pt-Ti alloy or intermetallic phases. Since the equilibrium solubility of Pt in a-phase Ti is about 1%, this implies that treatment has led to a metastable Pt-Ti alloy. It is presumably the presence of this new alloy, with attendant microstructural alterations caused by IBEST treatment, that has led to the increased durability.

VI. Summary

We have conducted surface modification and alloying experiments with various metals and bi-metal combinations. The goals are improved surface hardness, durability, and corrosion resistance. Samples were treated on the RHEPP-1 generator at Sandia National Laboratories with either a flashover or MAP ion source, the latter in a nitrogen beam mode. Surface modification of 440C stainless steel has resulted in as much as a six-fold increase in hardness as measured by nanoindentation, with attendant increases in durability. We believe this is due to carbide dispersal produced by the IBEST process. Mixing of Hf coatings into Al 6061 has led to substantial improvements in corrosion resistance as measured by electrochemical impedance spectroscopy. Mixing of a co-sputtered Pt-Ti layer into Ti-6Al-4V alloy has resulted in substantially improved surface durability. Further experiments are ongoing to understand the microstructural basis for these surface improvements.

VII. Acknowledgement

This work was supported by the United States Department of Energy under Contract DE-AC04-94AL85000. Sandia is a multi-program laboratory operated by Sandia Corporation, a Lockheed Martin Company, for the United States Department of Energy.

VIII. References

1. A. D. Pogrebnyak, Phys. Stat. Sol. (a) **117**, 17 (1990).

2. M. Nastasi, R. Fastow, J. Gyulai, J. W. Mayer, S. J. Plimpton, E. D. Wolf, and B. Manfred Ullrich, Nucl. Instr. Meth. Phys. Res. **B7/8**, 585 (1985).

3. R. W. Stinnett, R. G. Buchheit, F. A. Greulich, C. R. Hills, A. C. Kilgo, D. C. McIntyre, J. B Greenly, M. O. Thompson, G. P. Johnston, and D. J. Rej, Mat. Res. Soc. Symp. Proc. **316**, 521 (1994); R. W. Stinnett, R. G. Buchheit, E. L. Neau, M. T. Crawford, K. P. Lamppa, T. J. Renk, J. B Greenly, Ian Boyd, M. O. Thompson, and D. J. Rej, Proc. Tenth IEEE Pulsed Power Conf., Albuquerque, NM, July 3-6, 1995, W. Baker and G. Cooperstein, Eds., p.46. IBEST is a registered trademark of QM Technologies, Inc.

4. D. J. Johnson, J. P. Quintenz, and M. A. Sweeney, J. Appl. Phys. **57**, 794 (1985).

5. H. Yoshioka, S. Yoshida, A. Kawashima, K. Asami, and K. Hashimoto, Corrosion Sci. **26**, 795 (1986).

DISTRIBUTION

Unclassified Unlimited Release

1	MS9018	Central Technical Files, 8940-2
5	MS0899	Technical Library, 4916
2	MS0619	Review & Approval Desk, 12690 For DOE/OSTI

10 Prof. Rudolph G. Buchheit
The Ohio State University
Fontana Corrosion Center
Dept. of Materials Science and Engineering
477 Watts Hall
2041 College Rd.
Columbus, OH 43210-1187

10 Dr. Kenneth S. Grabowski
Code 6670, Building 74
Naval Research Laboratory
4555 Overlook Ave. SW
Washington, DC 20375

10 Prof. Michael O. Thompson
Department of Materials Science
Bard Hall
Cornell University
Ithaca, NY 14853

5 Dr. Walter M. Polansky
DOE/ER-32

Internal Distribution

1	MS1436	C. E. Meyers, 45234
10	MS0340	D. Cowell Senft, 1832
10	MS0340	N. R. Sorensen, 1832
5	MS0340	W. R. Cieslak
20	MS1182	T. J. Renk, 9521
10	MS1182	B. N. Turman, 9521
1	MS1188	R. A. Hamil, 9512
1	MS1190	D. L. Cook, 9500
1	MS1191	J. P. Quintenz, 9500